Vibro-acoustic analysis of composite plate-cavity systems via CUF finite elements

M. Cinefra[1], M. C. Moruzzi[2], S. Bagassi[2], E. Zappino[3], E. Carrera[3]

(1) Department of Mechanical, Mathematics and Management, Politecnico di Bari, Italy
(2) Department of Industrial Engineering, Università di Bologna, Italy
(3) Department of Mechanical and Aerospace, Politecnico di Torino, Italy

Author and address for Correspondence
Prof. Cinefra Maria
Associate professor,
Department of Mechanical, Mathematics and Management,
Politecnico di Bari,
Via Orabona, 4,
70125 Bari, Italy.
e.mail: maria.cinefra@poliba.it

Abstract

The vibro-acoustic problem of a plate made of an advanced material, like a composite one, backed to a fluid filled cavity represents an important issue for the automotive and the aerospace sector. In fact, the noise and the vibrations prediction and then mitigation leads to an essential increase in the structural safety of the system and in the passenger comfort. Over the last thirty years, a large amount of studies has been published about the vibratory characteristics of the structure-cavity systems and, thanks to these researches, the physical phenomena linked to the reduction of noise at low frequencies is well known. Although, there is a lack of accurate numerical models, valid for innovative materials, able to describe the complex kinematic behavior of new materials and so the structural response in the low frequency range. The aim of the this work is to develop reliable finite element models for vibro-acoustic analysis of structures made of advanced materials, coupled with fluid filled cavities. The structure is described according to the Carrera's Unified Formulation (CUF), in order to enhance a wide class of powerful refined 2D plate theories with a unique formulation. The fluid cavity is described with a standard pressure-based finite element formulation of the acoustic field. The numerical results are presented for the case of a plate backed to a fluid filled cavity. Different plate layouts, in terms of materials, are considered, and also different fluids for the cavity, in order to consider both the weak and the strong coupling interaction. The results are compared with the solutions obtained by Actran®, a commercial software based on finite element method.

1 Introduction

The aim of this work is to develop a numerical tool that is able to accurately predict the vibro-acoustic response of a plate-like structure backed to a fluid cavity at low frequencies.

The study of vibro-acoustic interaction between a plate-like structure and fluid cavity concerned different industrial sectors, as the automotive, the aeronautical and the space industry, both in terms of structural safety and users comfort. Literature reviews on vibro-acoustic phenomena for these sectors are those written by Qatu et al. [1] for the automotive field, by Dobrzynski [2] for the aeronautical field and by Pirk et al. [3] for the space industry. The vibro-acoustic problem at low frequency is well known both from the physical point of view and from the numerical as described by Atalla [4], although there is a lack of reliable numerical tools, valid for innovative materials with orthotropic properties, such as composite materials or metamaterials (microstructured materials with frequency dependent properties for acoustic applications, see the work of Cinefra et al. [5, 6, 7]). An inaccurate prediction in the plate dynamic response could lead to huge errors in the coupled solution and so in the structure borne noise prediction. Hence the need to fill the gap of numerical tools able to predict the vibro-acoustic response of a coupled plate-cavity system for innovative materials. In particular we will focus on the composite materials, so we have to deal with orthotropic properties and we consider different fibers orientations. Other works, as that of Danu et al. [8], studied the effects on the coupled plate-cavity system's solution of the inside structure of the composite material in terms of volume fraction. An overview of models adopted to solve the problem in sandwich structures is provided in [9]. Analyses on free vibration of a plate, without the air cavity are run by Gorman [10, 11] using the method of superposition in the case of weak coupling for an orthotropic plate. The same author Gorman et al. [12] studied the free vibration of symmetric cross-ply rectangular laminated plate. Gorman and Wei use, in their work, the superposition method. These works obtained accurate modal shapes. Other authors essayed a similar problem as Dalaei et al. [13] using the extended Kantorovich method and Yu et al. [14] using the the superposition technique for orthotropic plate with clamped and simply supported edges, finding the natural modes and the corresponding natural frequencies.

At low frequency Finite Element Method (FEM) could be used to solve the vibro-acoustic problem without high computational cost, in fact all the system components are small compared to the wavelength over the selected frequency range. In the work by De Rosa et al. [15] the fluid structural interactions are approached both from a theoretical and from a numerical point of view. The work by Dhandole et al. [16] looks for new methodology for vibro-acoustic FE model for a plate-cavity weak coupled system, with a focus on the structural dynamic model. For complex and huge geometry or for high frequency other methods as SEA (Synthetic Energy Analysis) are preferred. An other work by Madjlesi [17] studied the acoustic response of a cavity both at low and at high frequency range using FEM for the low frequency range and SEA for the high frequency range. SEA, FEM and hybrid methods are investigated by different authors, by Jiao et al. [18] on a rectangular enclosure with a flexible panel and in particular for aircraft structural model [19, 20].

In order to correctly reproduce the complex kinematic behaviour of the structure a powerful notation, the Carrera's Unified Formulation (CUF) [21], is used in this work, enabling a wide class of refined plate theories through the layer wise (LW) approach as described by Li et al. [22] for shell structures. The software MUL2[1] exploits this formulation.

The MUL2's solutions are compared with those obtained by Actran® software, a FEM based software produced by MSC Software Corporation. Actran® uses an equivalent single layer (ESL) approach to manage different layers and describes the plate kinematic. This simpler approach could lead to large errors in the solution if we use complex materials, like composite material. The ESL method inefficiency was already studied by Chronopoulos et al. [23], who built an updated ESL model time efficient and accurate for a wide frequency range. They also conducted an experimental validation of the model. Botshekanan Dehkordi et al. [24] use CUF in order to create a mixed LW/ESL models for the analysis of sandwich plates with composite faces. On the other hand, Actran® is already used to study complex vibro-acoustic problem at low frequency and so its process are well-known both from the authors and from the scientific community.[2] Studies on complex geometry with closed cavity, as an aircraft's fuselage or a car cabin, are conducted by Moruzzi et al. [25] and by Liu et al. [26] and on innovative materials plates, like metamaterials, by Cinefra et al. [6].

The aim of this work is to demonstrate the superiority of CUF plate finite elements based on LW approach in the vibro-acoustic analysis of composite structures. Many previous authors' works in literature [21, 22, 24, 27, 28, 29, 30, 31, 32] have shown the accuracy and computational efficiency of these elements in the pure mechanical analysis of composite plates by taking account the complex through-the thickness effects that arise in laminated structures; here, the authors demonstrate that the structural modeling significantly affects the vibroacoustic analysis at higher frequencies; in particular, the LW modelling of the plate permits to evaluate more accurately the dynamic response of the entire system when composite material and strong fluid-structure coupling are considered.
This work is the result of the researches carried out by the authors and of a previous work presented at the 3rd *Euro-Mediterranean Conference on Structural Dynamics and Vibroacoustics* [33]. In the first section of this work we describe the vibro-acoustic problem through its governing equations. Then the CUF is applied on the problem and described. In the next section we set the analysis parameters and so we describe and verify the FEM model. Finally, in the last section, the results are shown and explained.

---

[1]http://www.mul2.polito.it/
[2]https://www.mscsoftware.com/en-uk/product/actran-vibroacoustics

2 The vibro-acoustic problem

2.1 Governing equations

The plate-cavity problem can be led back to the classic system of a structure with an internal cavity. In this work the following hypotheses are assumed in order to resolve the vibro-acoustic problem:

- the fluid-structure system has a linear behavior;

- the deformation for the structure are small, in order to fulfil the continuum body hypothesis;

- the fluid is homogeneous, inviscid and irrotational compressible;

- the body forces, as the gravitational effects, are neglected.

The physical model in Figure 1 is the standard coupled system, with the structure domain Ω_s and its normal n_i^s and the fluid domain Ω_f and its normal n_i^f. The structure property is the density ρ_s, while the fluid has the reference density and the constant speed of sound ρ_f and c_f, respectively. On the structure the Dirchelet Γ_D^s, assigned displacement $\bar{s}_i$, Neumann boundary conditions Γ_N^s and a surface force f_i are applied. The fluid-structure interface is defined as Γ_{fs}. Moreover the linearized deformations tensor is denoted by ε_{ij} and the corresponding stress tensor σ_{ij}. Under these hypotheses we obtain the equations systems for the structure (1) and for the fluid (2):

$$\begin{cases} \sigma_{ij,j} = \rho_s \ddot{s}_i & \text{in } \Omega_s \\ \sigma_{ij} n_j^s = f_i & \text{in } \Gamma_N^s \\ s_i = \bar{s}_i & \text{in } \Gamma_D^s \\ \sigma_{ij} n_j^s = p\, n_i^f & \text{in } \Gamma_{fs} \,. \end{cases} \tag{1}$$

$$\begin{cases} p_{,ii} = \frac{1}{c_f^2} \ddot{p} & \text{in } \Omega_f \\ p_{,i} n_i^f = -\rho_f \ddot{s}_i n_i^f & \text{in } \Gamma_{fs} \\ p_{,i} n_i^f = 0 & \text{in } \Gamma_D^f \end{cases} \tag{2}$$

in which dots¨indicate the second derivative with respect to time.

2.2 Variational formulation

The previous *strong formulation* is expressed in terms of structural displacement s_i and fluid pressure p. In order to obtain the finite element formulation, we use the *weak formulation* of the differential equations, introducing an arbitrary time-independent test-function, so a virtual displacement. δ_{si}. We obtain the following equations (the first for the structure and the second for the fluid cavity):

$$\begin{cases} \int_{\Omega_s} \delta\varepsilon_{ij}\sigma_{ij} dV + \int_{\Omega_s} \delta s_i \rho_s \ddot{s}_i dV = \int_{\Gamma_N^s} \delta s_i f_i ds + \int_{\Gamma_{fs}} \delta s_i p\, n_i ds \\ \int_{\Omega_f} \delta p_{,i} p_{,i} dV + \int_{\Omega_f} \frac{1}{c_f^2} \delta p \ddot{p} dV = -\int_{\Gamma_{fs}} \delta p\, \rho_f \ddot{s}_i n_i ds \end{cases} \tag{3}$$

where the two last terms in the system represent the fluid-structure coupling.
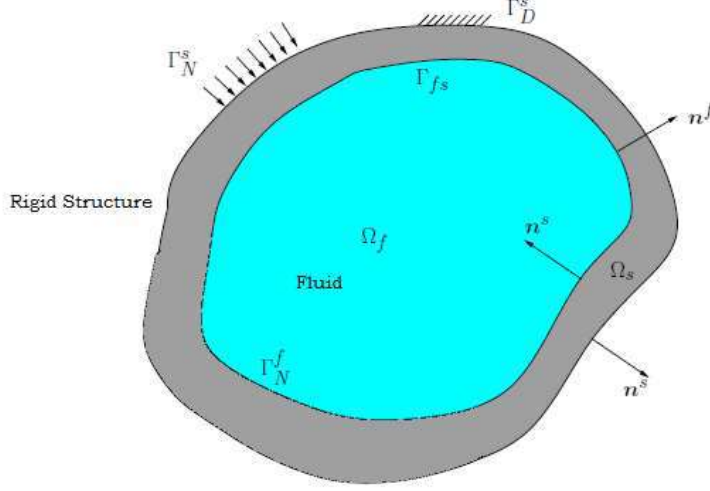
Figure 1: The coupled system domain, composed by a structure with an internal cavity.

3 Unified FE formulation

3.1 Preliminaries

We specify the generic structural coupled acoustic problem for a generic laminated plate made of an orthotropic material in contact with an acoustic cavity.

We can express the constitutive equation as:

$$\boldsymbol{\sigma} = \boldsymbol{C}\boldsymbol{\varepsilon} \tag{4}$$

where $\boldsymbol{C}$ is the matrix of elasticity coefficients. The stress tensor and strain tensor can be expressed thanks to the Voigt formulation:

$$\boldsymbol{\sigma}^T = \begin{bmatrix} \sigma_{xx} & \sigma_{yy} & \sigma_{zz} & \sigma_{yz} & \sigma_{xz} & \sigma_{xy} \end{bmatrix} \tag{5}$$

$$\boldsymbol{\varepsilon}^T = \begin{bmatrix} \varepsilon_{xx} & \varepsilon_{yy} & \varepsilon_{zz} & \varepsilon_{yz} & \varepsilon_{xz} & \varepsilon_{xy} \end{bmatrix} \tag{6}$$

and the matrix $\boldsymbol{C}$ in $(x,\ y,\ z)$ can be obtained from matrix $\boldsymbol{C}^*$ in the material reference system $(1,\ 2,\ 3)$, that is:

$$\boldsymbol{C}^* = \begin{bmatrix} C_{11} & C_{12} & C_{13} & 0 & 0 & 0 \\ C_{12} & C_{22} & C_{23} & 0 & 0 & 0 \\ C_{13} & C_{23} & C_{33} & 0 & 0 & 0 \\ 0 & 0 & 0 & C_{44} & 0 & 0 \\ 0 & 0 & 0 & 0 & C_{55} & 0 \\ 0 & 0 & 0 & 0 & 0 & C_{66} \end{bmatrix} \tag{7}$$

In order to refer the constitutive equation to the laminate reference system we use the rotation matrix $\boldsymbol{R}$:

$$\boldsymbol{C} = \boldsymbol{R}^T \boldsymbol{C}^* \boldsymbol{R} \tag{8}$$

Moreover the strain tensor could be obtained with the following equation:

$$\boldsymbol{\varepsilon} = \boldsymbol{D}\boldsymbol{\mathcal{U}} \tag{9}$$

5

where $\mathcal{U} = \begin{bmatrix} u & v & w \end{bmatrix}^T$ is the displacement vector and $\boldsymbol{D}$ is the matrix of differential operators:

$$\boldsymbol{D} = \begin{bmatrix} \frac{\partial}{\partial x} & 0 & 0 & 0 \\ 0 & \frac{\partial}{\partial y} & 0 & 0 \\ 0 & 0 & 0 & -\frac{\partial}{\partial x} \\ 0 & 0 & 0 & -\frac{\partial}{\partial y} \\ 0 & 0 & \frac{\partial}{\partial z} & 0 \\ \frac{\partial}{\partial z} & 0 & \frac{\partial}{\partial x} & 0 \\ 0 & \frac{\partial}{\partial z} & \frac{\partial}{\partial y} & 0 \\ 0 & 0 & 0 & -\frac{\partial}{\partial z} \end{bmatrix} \tag{10}$$

3.2   Carrera Unified Formulation (CUF)

We apply the Carrera Unified Formulation (CUF) in order to describe the displacement field [22, 27]:

$$\mathcal{U}(x, y, z, t) = F_\tau(z)\mathcal{U}_\tau(x, y, t) \tag{11}$$

in which $\tau = 1, ..., N$, so the order of the expansion goes from 1 to N. We divide the 3D problem in a 2D and a 1D problem which permits to build bi-dimensional shell models. The functions $F_\tau(z)$ depend only on the thickness coordinates z and so they are called thickness functions. The ESL (Equivalent Single Layer) models use a Taylor expansion centered on the mid-pane, with z that varies from $-h/2$ to $h/2$ (h is the whole plate thickness). The LW (Layers Wise) models suppose the variables independent in each layer and Lagrange polynomials are assumed as thickness functions. So z is defined as a local variable for the thickness of the k-th layer.

3.2.1   ESL and LW approach

In the equivalent-single-layer approach the composite structure is supposed to be an integral equivalent layer. The thickness expansion for the displacement $\mathcal{U}$ is obtained through Taylor polynomials:

$$\mathcal{U}(x, y, z, t) = F_0\mathcal{U}_0 + F_1\mathcal{U}_1 + ... + F_N\mathcal{U}_N = F_\tau(z)\mathcal{U}(x, y, t) \tag{12}$$

in which $F_0 = z^0 = 1$, $F_1 = z^1$, ..., $F_N = z^N$ so $F_\tau = z^\tau$. These theories are usually accurate to estimate the global laminate response, but they became unsuitable if stresses at ply level are required. Moreover they can be inaccurate when there are localized loads or in case of high anisotropy. Commercial software, as Actran®, are usually based on ESL theory with order $N = 1$, such as the First-order Shear Deformation Theory (FSDT).

On the other hand, the layer-wise approach supposes the composite structure composed by independent layers. In this way it is possible to have a 3D description of stress-strain state in the material. The method is described by the following equation:

$$\mathcal{U}^k(x, y, z, t) = F_\tau(x_k)\mathcal{U}_\tau^k(x, y, t) \tag{13}$$

where F_τ^k are defined as Lagrange interpolation polynomials:

$$F_\tau^k(\zeta_k) = \prod_{i=0, i \neq \tau}^{N} \frac{\zeta_k - \zeta_{k_i}}{\zeta_{k_\tau} - \zeta_{k_i}} \tag{14}$$

in which $-1 \leq \zeta_k \leq 1$ is the adimensional thickness coordinate in the layer k. For example $\zeta_{k_0} = -1$ represents the bottom surface of the k-th layer, while $\zeta_{k_N} = 1$ the top surface.
The continuity of the displacements at the interface of two neighboring layers must be satisfied [27].

3.2.2 Finite element approximation

We apply the FE approximation to the coupled problem and we introduce the shape functions N_i to approximate the displacements (structural variable) and pressure (fluid variable) functions:

$$\mathcal{U}_\tau^k(x,\ y,\ t) = N_i(x,\ y)U_\tau^k(t) \tag{15}$$

$$p(x,\ y,\ z,\ t) = N_i(x,\ y,\ z)P_i(t) \tag{16}$$

where $i = 1,\ ...,\ n^s$ for the structural variables and $i = 1,\ ...,\ n^p$ for fluid variables. n^s is the number of nodes of the 2D structural element and n^p is the number of nodes of the 3D fluid element. The term U contains the nodal value derived from the CUF model for the plate sub-problem and therefore we can write the following equation from Equations (11) and (15):

$$\mathcal{U}_\tau^k(x,\ y,\ z,\ t) = F_\tau(z)N_i(x,\ y)U_\tau^k(t) \tag{17}$$

According to the choice of the functions F_τ, we can have the ESL or the LW approach. In this work, only the layer-wise models are considered in the framework of the MUL2 software, while the commercial software Actran® is that one based on ESL approach.

LWN is the notation adopted for LW models, where LW define the use of a LW description and N indicates the order of the expansion of the theory.

3.3 Fundamental matrices

The structural mass matrix $\boldsymbol{M}$, the structural stiffness matrix $\boldsymbol{K}$, the load vector $\boldsymbol{F}$, the fluid coupling matrix $\boldsymbol{S}$, the fluid mass matrix $\boldsymbol{Q}$ and the fluid stiffness matrix $\boldsymbol{H}$ are obtained in terms of fundamental nuclei, which are independent from expansion order in the thickness direction.

We define the structural stiffness matrix as:

$$\int_{\Omega_s^k} \delta\mathcal{U}^{kT}\boldsymbol{D}^T\boldsymbol{C}^k\boldsymbol{D}\mathcal{U}^k dV = \delta U_{sj}^{kT}\boldsymbol{K}_{sij\tau}^k U_{\tau i}^k \tag{18}$$

in which the fundamental nuclei is a 3x3 matrix defined as:

$$\boldsymbol{K}_{\tau sij\tau}^k = \int_{\Omega_s^k} N_j(x,y)F_s(z)\boldsymbol{D}^T\boldsymbol{C}^k\boldsymbol{D}F_\tau(z)N_i(x,y)dV \tag{19}$$

In a similar way we obtain the structural external load vector:

$$\int_{\Sigma^k} \delta\mathcal{U}^{kT}\boldsymbol{f}_m^k ds = \delta U_{sj}^{kT}\boldsymbol{F}_{sj}^k \tag{20}$$

in which the external load is $f_m^k(x,y) = [f_u(x,y)f_v(x,y)f_w(x,y)]^T$ applied at the coordinate z_l. The fundamental nuclei is a 3x1 matrix defined as:

$$\boldsymbol{F}_{sj}^k = F_s(z_l)\int_{\Sigma^k} N_j(x,y)\,f_m^k(x,y)\,ds \tag{21}$$

where Σ^k is the reference area for the layer k that, in this work, coincide with the area of the interface between the plate and the fluid volume Σ_{fs}.

The fluid-structure coupling matrix is expressed in terms of fundamental nuclei by the following equation:

$$\int_{\Sigma_{fs}} \delta \boldsymbol{\mathcal{U}}^{kT} p\,\boldsymbol{n}\,ds = \delta \boldsymbol{U}_{sj}^{kT} \boldsymbol{S}_{sij}^{k} \boldsymbol{P}_i \tag{22}$$

in which the fluid coupling nucleus is a 3x1 matrix:

$$\boldsymbol{S}_{sij}^{k} = F_s(z_{fs}) \int_{\Sigma_{fs}} N_j(x,y) N_i(x,y)\,\boldsymbol{n}\,ds \tag{23}$$

and $\boldsymbol{n}$ is the normal to the fluid-structure interface.
The structural mass matrix derives from the virtual work done by the inertial load:

$$\int_{\Omega_s^k} \delta \boldsymbol{\mathcal{U}}^{kT} \rho_s^k \ddot{\boldsymbol{\mathcal{U}}}^{k} dV = \delta \boldsymbol{U}_{sj}^{kT} \boldsymbol{M}_{\tau sij}^{k} \ddot{\boldsymbol{U}}_{\tau i}^{k} \tag{24}$$

in which the fundamental nucleus is defined as:

$$\boldsymbol{M}_{\tau sij}^{k} = \int_{\Omega_s^k} N_j(x,y) F_s(z) \rho_s^k F_\tau(z) N_i(x,y)\,dV \tag{25}$$

The fluid internal work is obtained as the acoustic stiffness matrix:

$$\int_{\Omega_f} \delta p_{,l}\, p_{,l}\,dV = \delta \boldsymbol{P}_j^T \boldsymbol{H}_{ij} \boldsymbol{P}_i \tag{26}$$

in which summation index l has been introduced and the fundamental nucleus is defined as:

$$\boldsymbol{H}_{ij} = \int_{\Omega_f} N_{j,l}(x,y,z) N_{i,l}(x,y,z)\,dV \tag{27}$$

Finally the fluid inertial work is expressed in terms of fundamental nuclei, so we obtain the acoustic mass matrix:

$$\frac{1}{c_f^2} \int_{\Omega_f} \delta p\, \ddot{p}\,dV = \delta \boldsymbol{P}_j^T \boldsymbol{Q}_{ij} \ddot{\boldsymbol{P}}_i \tag{28}$$

where the fundamental nucleus is equal to:

$$\boldsymbol{Q}_{ij} = \int_{\Omega_f} N_j(x,y,z) N_i(x,y,z)\,dV \tag{29}$$

Ones the fundamental nuclei are expanded on the indexes τ, s, i and j, we obtain the final equations for the coupled problem that include the FE approximation and the CUF for the structure:

$$\begin{bmatrix} \boldsymbol{M} & 0 \\ -\rho_f \boldsymbol{S}^T & \boldsymbol{Q} \end{bmatrix} \cdot \begin{Bmatrix} \ddot{\boldsymbol{U}} \\ \ddot{\boldsymbol{P}} \end{Bmatrix} + \begin{bmatrix} \boldsymbol{K} & \boldsymbol{S} \\ 0 & \boldsymbol{H} \end{bmatrix} \cdot \begin{Bmatrix} \boldsymbol{U} \\ \boldsymbol{P} \end{Bmatrix} = \begin{Bmatrix} \boldsymbol{F} \\ 0 \end{Bmatrix} \tag{30}$$

4 Model validations and analysis

4.1 Acoustic coupling

The coupling between the fluid and the structure depends on the fluid nature and on the structure acoustic properties. We can characterize the amount of coupling, defining the following parameter:

$$\beta_c = \frac{\rho_o c_0}{\rho_s h_s \omega_s} \tag{31}$$

in which ρ_0 and c_0 are the fluid density and sound speed respectively, ρ_s the density of the structure, h_s the characteristic thickness of the structure and ω_s its first natural frequency.

Using the parameter β_c we can estimate the strength of the fluid-structure interaction [34]. There are two general cases:

- for $\beta_c \ll 1$ there is a weak coupling interaction. In general, this is the case of a low density fluid, as air. For weak coupling, we can calculate only the structural vibratory response in order to fully determine the coupled solution and then superpose it to the modal fluid behaviour;

- for $\beta_c \gg 1$ there is a strong coupling and this is the case of high density fluid, as water. The fluid modifies the vibratory and acoustic response of the structure. Therefore we must consider the fluid coupling in order to determine the coupled solution, resolving simultaneously the coupled equations governing the wave propagation in the fluid and in the structure.

In the following analyses we consider these two different cases: a weak coupling with a cavity filled with air $\beta_c \simeq 0.3085$ and a strong coupling with a cavity filled with water $\beta_c \simeq 1388.88$.

4.2   Model and process

As previous described we want to compare the results given by the MUL2 software with those of the commercial software Actran®.

We will deal with a square plate 1x1 m^2 with a thickness equal to 0.01 m. The mesh is composed by 20×20 linear plate elements in Actran® and 10×10 nine-nodes plate elements in MUL2. The plate material can be:

- an isotropic material (aluminium) with the following properties: Young's modulus $E_s = 70\ GPa$, mass density $\rho_s = 2700\ kg/m^3$ and Poisson's ratio $\nu = 0.35$;

- an orthotropic material (Young's modulus $E_1 = 25\ GPa$, $E_2 = E_3 = 1\ GPa$, shear modulus $G_{13} = G_{23} = 0.5\ GPa$, $G_{12} = 0.2\ GPa$, Poisson's ratio $\nu_{13} = \nu_{23} = \nu_{12} = 0.25$ and mass density $\rho_s = 1000\ kg/m^3$) composed by three layers with the following lamination $0^o/90^o/0^o$.

The cavity is a cube of 1x1x1 m^3 composed by $20 \times 20 \times 20$ linear 3D elements in Actran® and $10 \times 10 \times 10$ 3D parabolic elements in MUL2. The fluid can be:

- air (weak coupling) with the following properties: speed of sound $c_f = 343\ m/s$ and mass density $\rho_f = 1.2\ kg/m^3$;

- water (strong coupling) with the the following properties: speed of sound $c_f = 1500\ m/s$ and mass density $\rho_f = 1000\ kg/m^3$.

The plate is placed on the top of the cavity and its edges are simply supported and an interface between the plate (structure) and the cavity (fluid) is created. The plate-cavity model is shown in Figure 2 with its reference system. A constant amplitude force excitation of 1 N is applied on the plate at the point $A = (0.25\ m,\ 0.35\ m,\ 1.0\ m)$. The analyses are performed at low frequency range 0-300 Hz. The measurement locations of the pressure are the points $B = (0.75\ m,\ 0.75\ m,\ 0.75\ m)$ and $C = (0.35\ m,\ 0.70\ m,\ 0.65\ m)$ inside the cavity (virtual microphones).
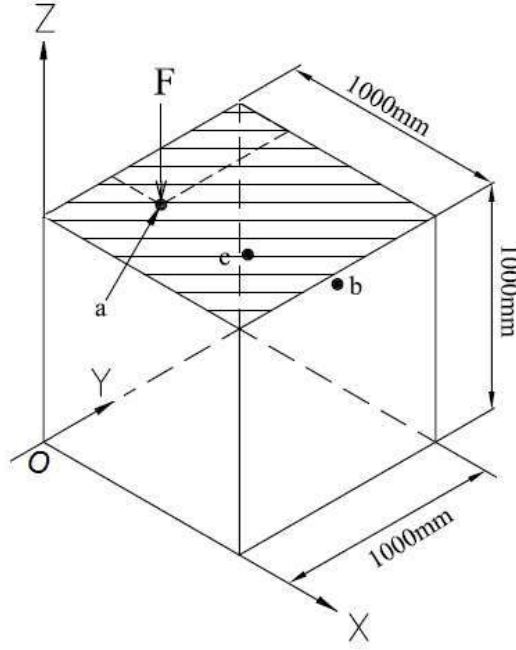
9

Figure 2: The plate-cavity coupled system.

Summing up, we have two materials for the plate (one isotropic and one multi-layers orthotropic material) and two materials for the cavity (air and water). On the plate a concentrated load is applied and the analysis is performed from $0\ Hz$ to $300\ Hz$. The model is composed by three components: the plate (2D elements), the cavity (3D elements) and the fluid-structure interface (2D elements).

In order to have a good level of accuracy, Actran$^{\circledR}$ suggests to have from 3 to 6 elements per wavelength for quadratic interpolation elements. The maximum element size h is expressed by the following equation:

$$h = \frac{\lambda_{min}}{k} \tag{32}$$

in which k is the chosen criterion and λ_{min} the smallest wavelength in our problem. This last parameter depends on the material properties and on the max frequency in the problem. All the elements with their different materials, both for the structure and for the cavity, largely satisfy the criterion of $k = 6$ for a maximum frequency equal to $300\ Hz$ as reported in Table 1.[3]

Table 1: The elements per wavelength for each material used in the analyses from $0\ Hz$ to $300\ Hz$.

	Structure		Cavity	
Material	Aluminium	Orthotropic	Air	Water
Element size h [m]	0.01	0.01	0.1	0.1
Minimum wavelength λ_{min} [m]	0.57	1.05	1.13	5.0
Elements per wavelength k	105	57	113	500

---

[3]For the orthotropic material we consider the strictest direction in order to keep a conservative approach.

Table 2: First 10 natural frequencies [Hz] obtained with the analytical solution and the CUF, and the relative error.

Frequency	Analytical [Hz]	CUF [Hz]	Relative error [%]
1	0	0	0
2	171.5	171.5	0
3	171.5	171.5	0
4	171.5	171.5	0
5	242.54	242.54	0
6	242.54	242.54	0
7	242.54	242.54	0
8	297.05	297.05	0
9	343	343.04	0.02
10	343	343.04	0.02

4.3 MUL2 validation

4.3.1 Fluid

The MUL2 code must be validated, so we start from the fluid with a cubic cavity. We will compare the analytical solution of the problem with that obtained by the software in terms of natural frequencies. The analytical solution of the eigenvalue problem for this simple geometry is known and is given by the following relation:

$$\omega_{ijk} = \sqrt{c_f^2 \cdot \left[\left(\frac{i\pi}{a}\right)^2 + \left(\frac{j\pi}{b}\right)^2 + \left(\frac{k\pi}{c}\right)^2 \right]} \tag{33}$$

in which a, b and c are the three geometrical dimensions of the cube, c_f the fluid's speed of sound, i, j and k are the modal order along the three axes.

The acoustic element considered is a cubic rigid walled cavity 1x1x1 m with 10x10x10 27-node hexahedral element. The cubic cavity is filled with air (density $\rho_f = 1.225 \ kg/m^3$ and speed of sound $c_f = 343 \ m/s$). We consider the first 10 natural frequencies, the analytical, the numerical results and the relative errors are reported in Table 2. The results obtained with the FE code based on the Unified Formulation are in perfect agreement with the analytical ones.

4.3.2 Structure

The structural validation for the software MUL2 is already available in literature for an isotropic plate and for an orthotropic one.

In the work by Ferreira et al. [29] validations of MUL2 for an isotropic plate are performed. The paper estimate and validate, through numerical experiments, the capability and efficiency of CUF technique for static and dynamic problems, moreover the numerical accuracy and convergence are thoughtfully examined. The case of composite structures is carried out by Carrera et al. in [30, 31, 32, 35].

4.4 Coupled model

Despite the high reliability of Actran$^{\circledR}$, we validate our coupled model in order to eliminate any possible error. In this test, the cavity-plate we consider is represented in Figure 2. The mechanical properties of the structure are as follows: Young's Modulus $E = 70\ GPa$, mass density $\rho_s = 2700\ kg/m^3$ and Poisson's ratio $\nu = 0.35$. The cavity is filled with air with the following properties: speed of sound $c = 343\ m/s$, mass density $\rho_f = 1225\ kg/m^3$. The coupled system is excited using a constant structural point force of 1 N, applied in the point A, over the entire frequency range of 0-300 Hz at one of the off-center structural nodes on the simply supported plate. We measure the fluid pressure in the point B and C. The solution is compared with that obtained by Puri et al. [36] via implicit moment matching.

In Figure 3 we compare the two solutions in terms of acoustic pressure. The validating process has been passed. In fact, the main peaks of the solution process highly coincide the the solution in literature, and this is enough important for the validating process design.
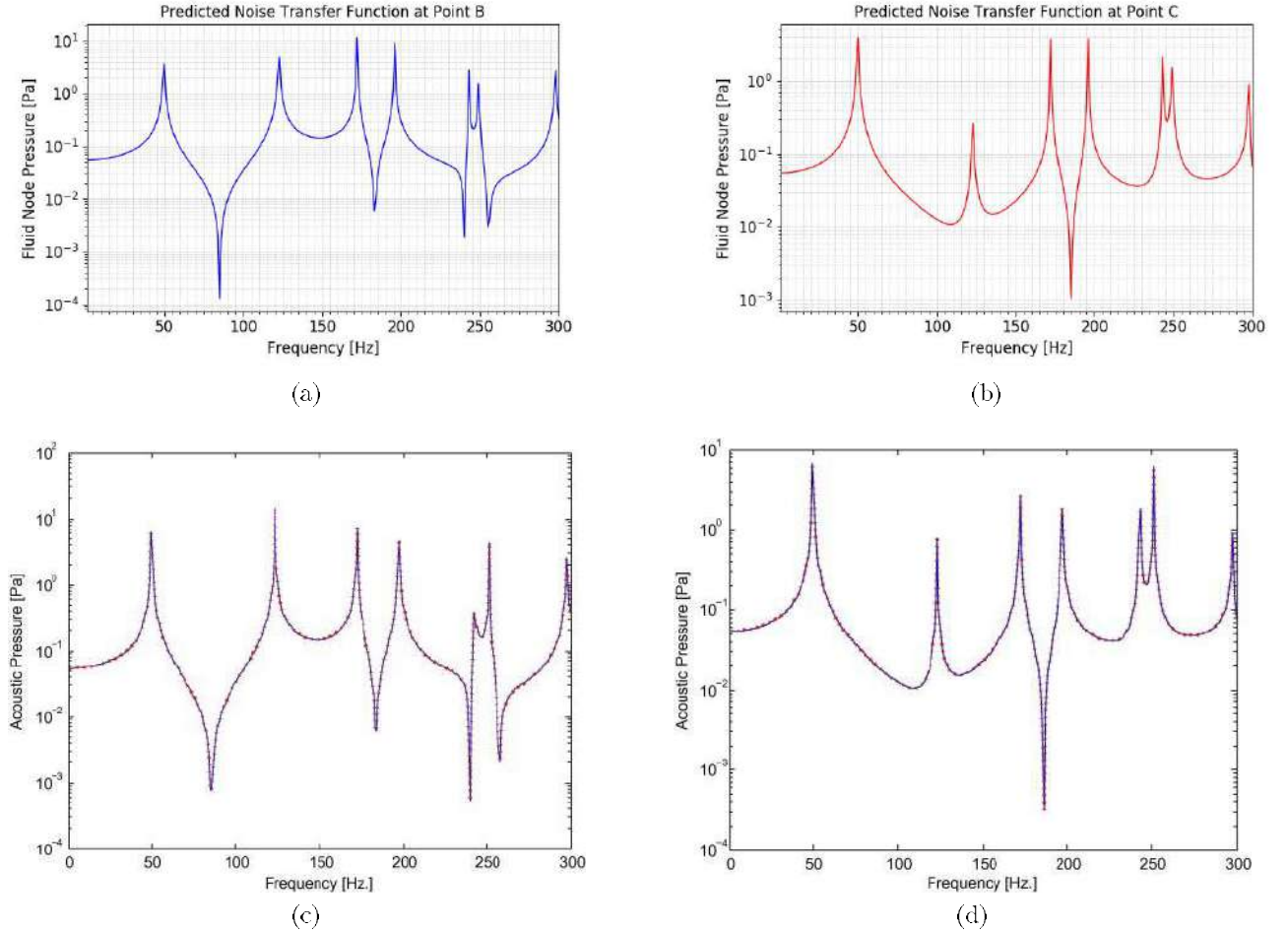

Figure 3: The acoustic pressure [Pa] comparison in order to validate the Actran's coupled model. (a) Actran Point B. (b) Actran Point C. (c) Puri et al. [36] Point B. (d) Puri et al. [36] Point C.

4.5 Structural validation

In order to compare the solution obtained with MUL2 and Actran®, we have to validate the structural behavior in order to eliminate or understand any structural responsibility in the possible differences of the two solutions. Therefore, we consider only the previous plate, without the cavity, on which we applied the concentrated load in the frequency range 0-300 Hz. We will test four different situations, changing the plate material (isotropic or orthotropic with two different laminations) and the boundary conditions applied on the edges (simply supported or clamped). The simply supported edges limit the vertical displacement, so $w = 0$. The clamped edges boundary conditions limit all the displacements, so $u = 0$, $v = 0$ and $w = 0$.

In order to estimate the displacement in a chosen point (0.25 m, 0.35 m) the software MUL2 uses different polynomial-grade displacement function (LW approach), while Actran® exploits an ESL approach.

4.5.1 Isotropic material

Figure 4 shows that, for the simply supported edges boundary conditions, the solution by Actran® and MUL2 with LW2 theory (or higher) are comparable. The difference slightly increases with a clamped boundary condition, but it remains comparable. So, we expect a small difference for the coupled solution caused by the structure.

The maximum local peak in Figure 4 represents the natural frequency of the plates. For example for the isotropic plate with simply supported edges we have four natural frequencies (in the 0-300 Hz range): 49 Hz, 123 Hz, 197 Hz and 246 Hz. To each natural frequency, a mode which control the plate's dynamic behaviour corresponds [37]. The modes for the four natural frequencies are shown in Figure 5. Different natural frequencies and modes exist for the clamped edges case and for the orthotropic plate. The natural frequencies of the clamped edges case are higher than those of the simply supported edges case. In fact, the clamped edges increase the plate stiffness [4]. Moreover the boundary conditions do not modify the previous small differences between the two software.
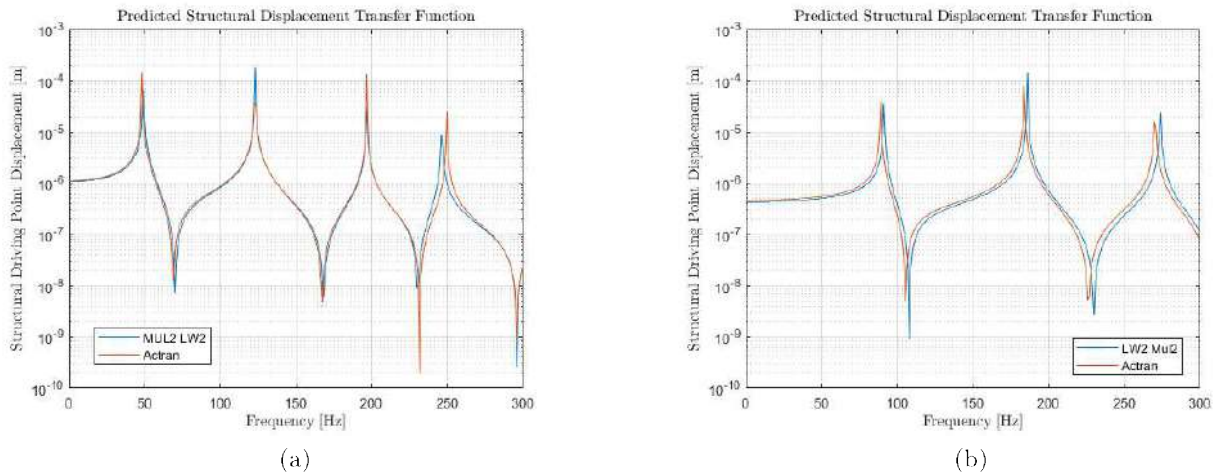

Figure 4: Displacement at (0.25 m, 0.35 m) for the isotropic plate. (a) Simply supported edges. (b) Clamped edges.
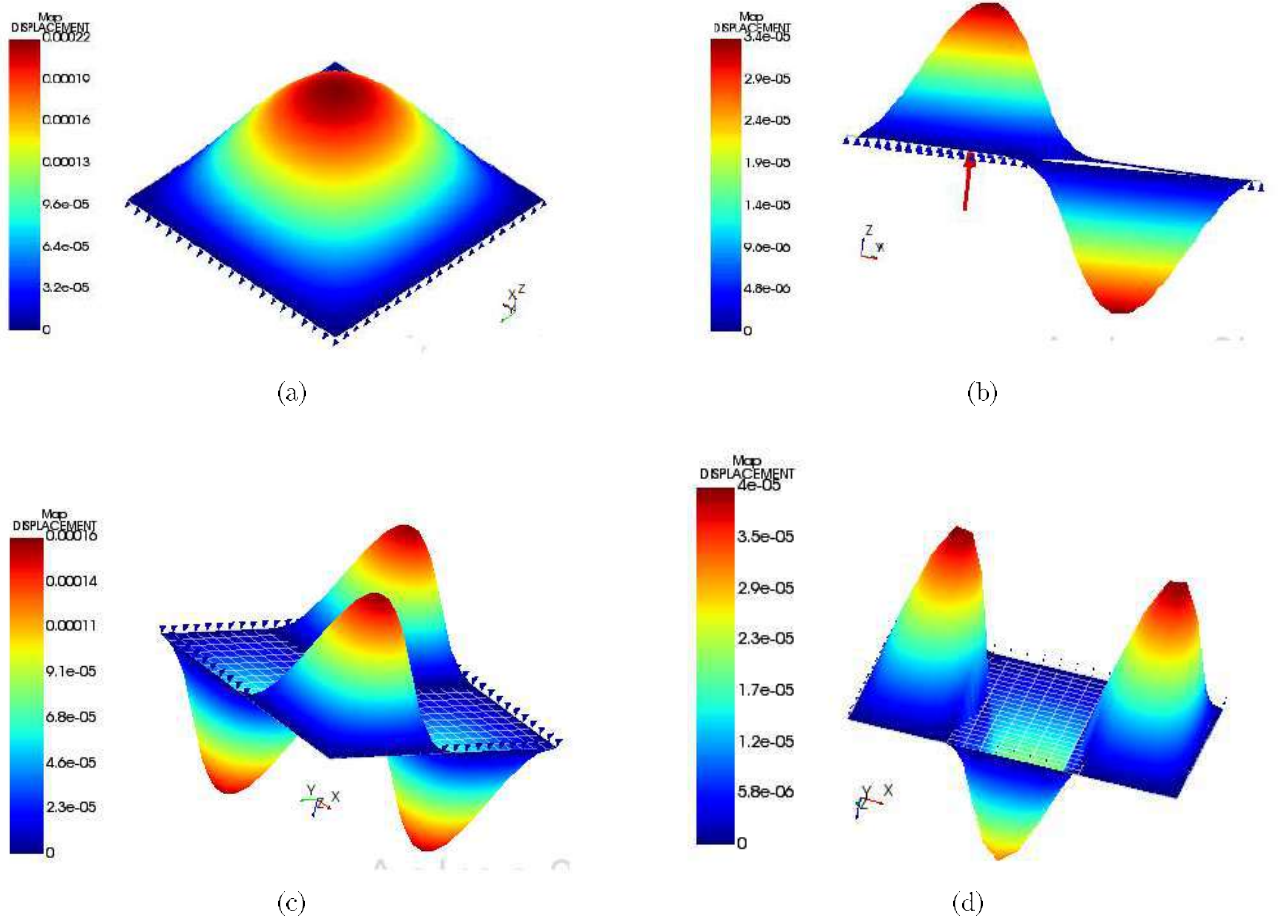
Figure 5: Plate modes. (a) 49 *Hz*. (b) 123 *Hz*. (c) 197 *Hz*. (d) 246 *Hz*.

4.5.2 Orthotropic material

As we can see in Figure 6, the differences between the software increase. The LW approach used by MUL2, in particular LW2 model, is able to capture the complex dynamic behaviour of the structure, while the ESL approach, used by Actran®, approximate the properties of the multi-layers laminate with the average properties. The error of the ESL approach increases with the frequency. This great difference will interfere with the solution of the coupled problem. The solutions problem on the orthotropic plate vibrations is already studied in different works [13, 38, 39], in particular for clamped edges that lead to an increase in the plate stiffness [40]. Anyway, in this case, we can conclude that the boundary conditions don't affect the accuracy of the solution.

4.6 Coupled system

At last, we can perform the analyses on the coupled system. The results will be separated in the next section for the weak and the strong coupling. For the isotropic plate we will study the effect of the increase in the thickness of the plate. Moreover we will study the mesh variation effect on the Actran® solution compared with the MUL2 solution. The results are reported in terms of fluid pressure in Pascal in the point B and C where we placed two virtual microphones.

14
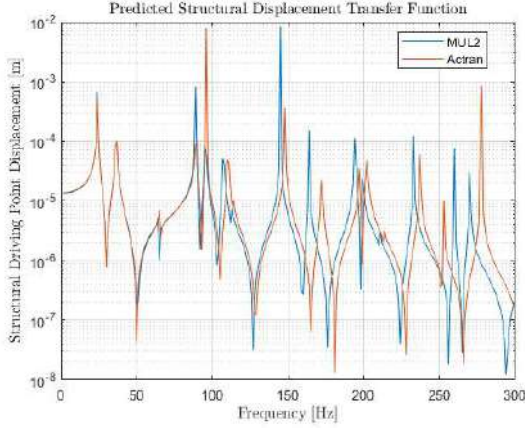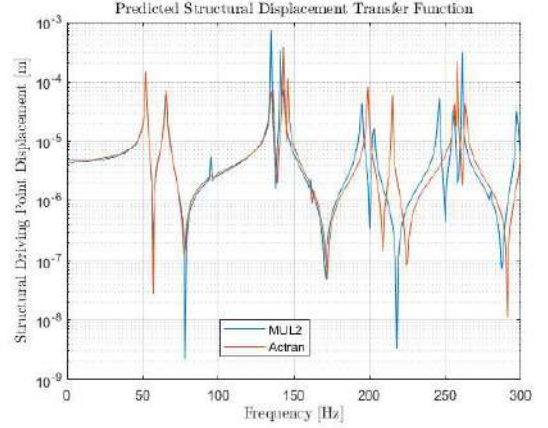
Figure 6: Displacement at (0.25 m, 0.35 m) for the orthotropic plate with different lamination and boundary conditions. (a) $0^o/90^o/0^o$, simply supported edges. (b) $0^o/90^o/0^o$, clamped edges.

5   Results

5.1   Weak coupling

In the weak coupling case the cavity is filled with air ($\rho_f = 1.2 \ kg/m^3$ and $c_f = 343 \ m/s$).

The following cases will be analyzed for the weak coupling:
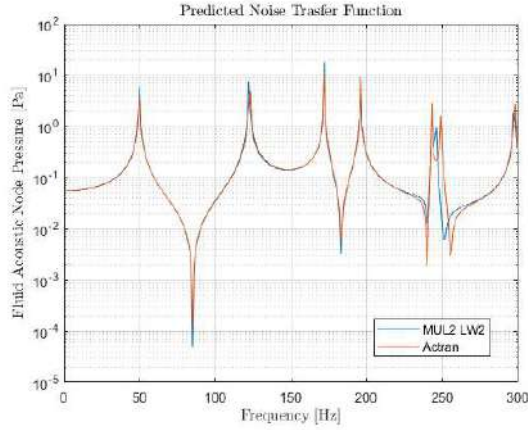
- isotropic plate;

- orthotropic plate.

5.1.1   Isotropic plate

The compared results by Actran® and by MUL2, in terms of pressure, for the isotropic model (isotropic plate with thickness $t = 0.01 \ m$ and simply supported edges) are reported in Figure 7, for the LW2 and LW3 approaches.

It can be observed that there are not significant differences in the respective noise transfer functions between the two software, despite the expansion order is increasing. As expected, more it increases, more time is necessary to compute the solution; so, we will continue to use the LW2 model in the following analyses.
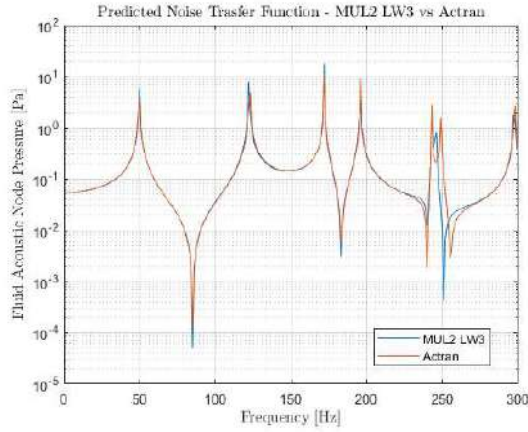
5.1.2   Orthotropic plate

The results in Figure 8 confirm the differences, in particular at high frequencies, between Actran® and MUL2 software, caused by the different structural behaviour. Indeed the ESL approach, despite the lower computational cost due to the small number of variables, fails in understand the dynamic response of the system.
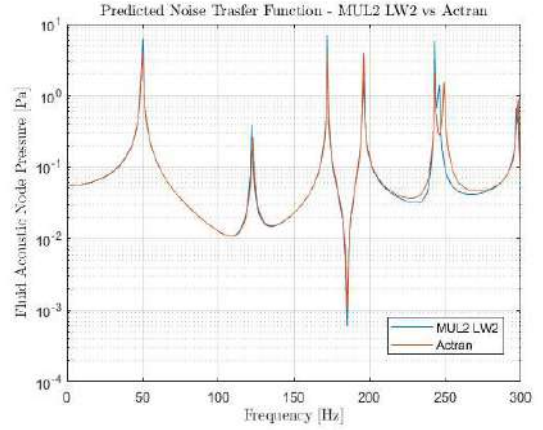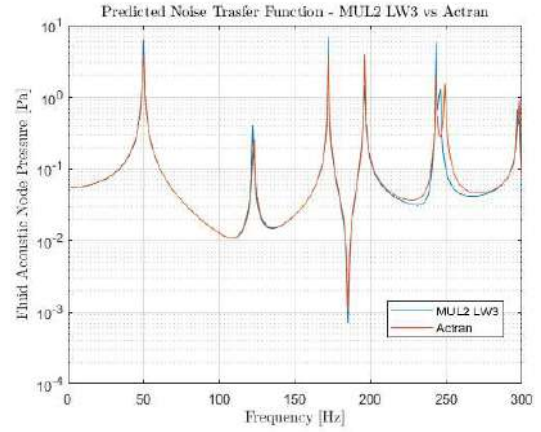
Figure 7: Fluid node pressure for a isotropic plate with simply supported edges backed to an air cavity (a) LW2 point B (b) LW2 point C. (c) LW3 point B. (d) LW3 point C.

5.2   Remarks

The differences in the FRF response between the MUL2, with an LW2 approach, and the Actran® models are evident only for the orthotropic case, particularly at high frequencies.

Moreover we can also view and verify that the resonance frequency in case of weak coupling can be obtained through the superposition of the modal vibration of the plate and of the fluid cavity. So we add three new modes at 171 Hz, 242 Hz and 297 Hz.

5.3   Strong coupling

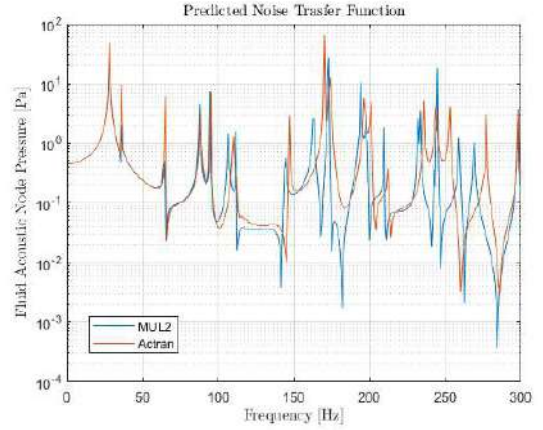Water ($\rho_f = 1000 \ kg/m^3$ and $c_f = 1500 \ m/s$) fills the cavity and leads to a strong coupling interaction between the cavity and the plate.

We will test two different cases:

- isotropic plate;

16
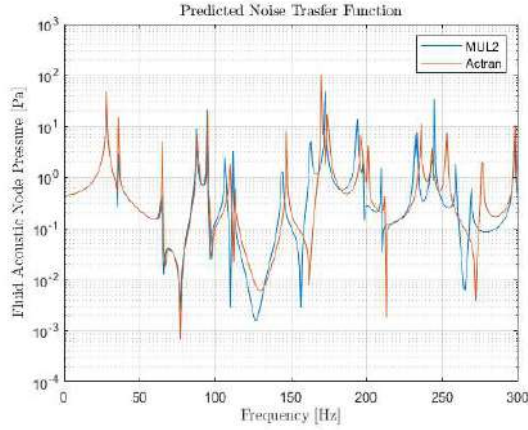
Figure 8: Fluid node pressure for orthotropic plate backed to an air cavity ($0^o/90^o/0^o$, simply supported edges). (a) Point B. (b) Point C.
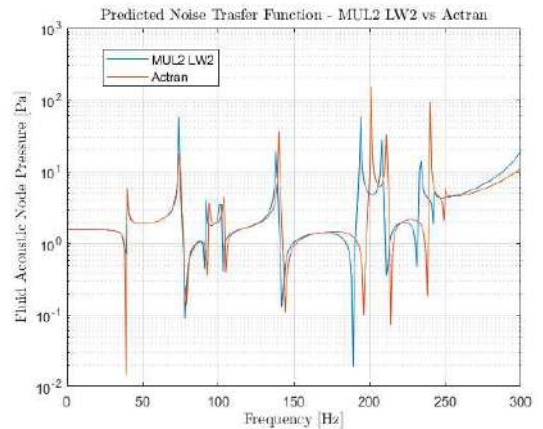
- orthotropic plate.

5.3.1 Isotropic plate

We have to decide the order of the expansion to discretize the plate thickness and, as in the previous case, we use a LW2 model. In fact, from previous studies [41], the LW2 approach is already able to guarantee good accuracy for thick plates.

The first case is the isotropic plate, with simply supported edges and a thickness equal to $t = 0.01\ m$ in a water filled cavity. The solution in terms of acoustic pressure is reported in Figure 9. As expected, the mean pressure in this case is higher than in the previous case with air.
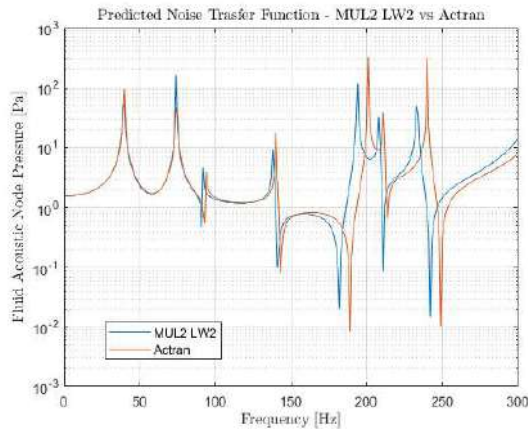
Figure 9: Fluid node pressure for a isotropic plate with simply supported edges backed to a water cavity (a) point B (b) point C.

The differences between the two software are negligible at low frequencies, but they begin to rise in the second half on the frequency range. So the stronger coupling lightly affects the accuracy of the solution

and we can note that the resonance peaks found with Actran[®] are higher than MUL2 one; therefore, we can reasonably conclude that the MUL2 solution is more accurate.

5.3.2 Orthotropic plate

The comments on the solutions shown in Figure 10 are the same of those for the weak coupling case, although due to the strong coupling there is an increase in the detachment between the two solutions. In fact, the structural approximation of the ESL models strongly influences the solution of the coupled system. So there are significant differences, in particular at high frequencies, between the MUL2 and Actran[®] solutions.
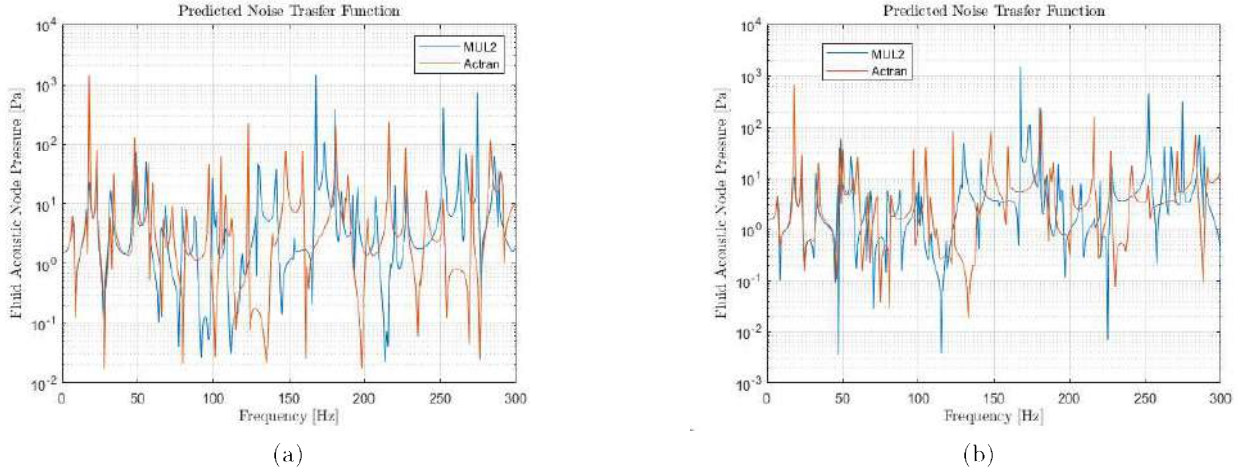

(a)   (b)

Figure 10: Fluid node pressure at point B for an orthotropic plate backed to a water cavity ($0^o/90^o/0^o$, simply supported edges). (a) Point B. (b) Point C.

5.3.3 Remarks

The high density fluid highlights every single modal contribution. The natural frequency of the system are not the superposition of the plate and cavity modes, as in weak coupling case. The term in the Equation (30) of the fluid mass $-\rho_f S^T$ is not negligible due to the high density of the fluid.

The differences between the two software rise with the coupling strength of the system, in particular at high frequencies.

5.4 Mesh variation

We increase the mesh of the Actran[®] model in order to demonstrate that the Actran[®] solution tends to the MUL2 solution, which represents the correct solution, due to its advanced theory.

We consider the most adverse case: strong coupling (water filled cavity) and the orthotropic plate. The MUL2 mesh is unchanged, while we increase the number of elements used in Actran[®] to discretize the structure. For the Actran[®] structure, we consider the following mesh: 20×20 and 80×80.

From Figure 11 we can observe that, for a 20×20 mesh, the two solutions begin to overlap at low

frequencies. For a 80×80 mesh the two solutions are almost the same for higher frequencies too. So the Actran® solution tends to the MUL2 solution if we increase the Actran®'s structural mesh. Therefore, we can reasonably associate this effect to the modelling of the fluid-structure interface that in MUL2 appears to be more accurate.
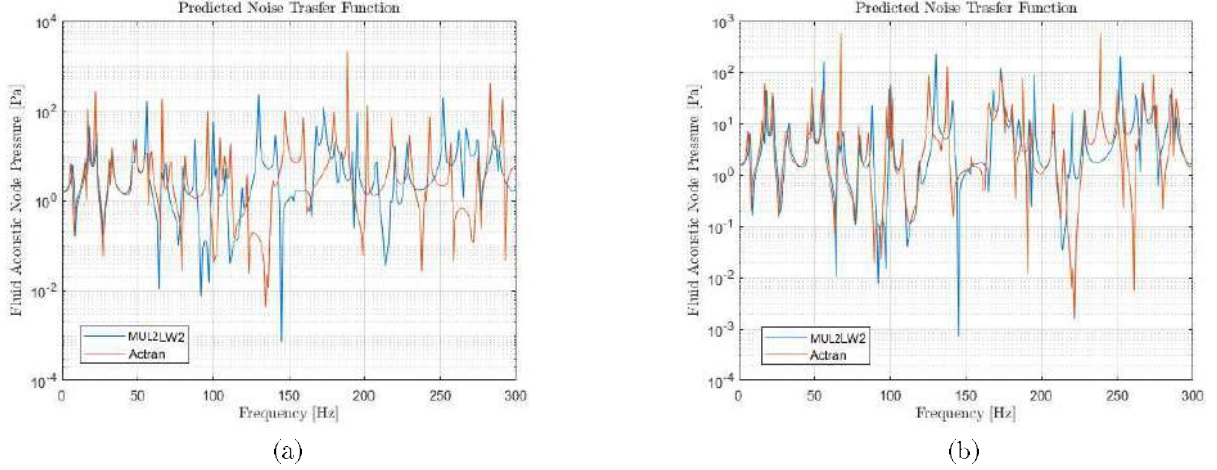

Figure 11: Fluid node pressure for an orthotropic plate backed to a water cavity and different structural mesh. (a) 20x20 elements (b) 80x80 elements.

6 Concluding remarks

The current work focus is to predict the vibro-acoustic behavior of composite structures by means of advanced finite elements based on CUF. In fact, the prediction of noise due to the fluid-structure interaction (structure borne noise) interest different industrial sector and so we need new numerical tools which deal with advanced material too.

The objective of this work is to validate the MUL2 software, developed by MUL2 research group in the *Politecinco di Torino* and based on CUF, for the vibro-acoustic analysis by comparing the results through commercial software, like Actran®. The results reward the MUL2 software approach, in fact the solutions have a better accuracy than those obtained by Actran®. At low frequency there are small differences between the two software, while, due to the frequency dependent behaviour of the problem, and so of the solutions, for higher frequency the discrepancies increase, in particular for the strong coupling case, due to the reduced wavelength, and for the orthotropic material. This differences are generated by the different approach exploited by Actran® and MUL2, ESL and LW respectively. In fact, the LW method takes into account multi-layer effects that the ESL method does not cover. Hence, the increasing of the differences for a composite plate, where the Actran®'s average properties do not capture the complex kinematic behaviour of the plate and for the water filled cavity, where the coupling effects are stronger; while these differences may be considered negligible in the case of isotropic material.

At the current state of the art, there are few works reporting LW methodology for the vibro-acoustic problem, in order to have a better description of the structural behaviour, with an insight to new advanced materials. In literature, most of research is typically focused in a numerical model with an ESL approach. Therefore the innovative features of the presented work is the integration of CUF inside a coupled problem in order to estimate the correct frequency response function, in terms of acoustic

pressure, for not-isotropic material too. So a validation of both dynamic and acoustic numerical model is conducted.

This work is only the first step in applying a more accurate structural model for a plate-cavity vibro-acoustic problem. Different future developments could be implemented and studied:

- to expand the model to new structural shapes, as curved structures, and to the computation of useful parameters such as transmission loss and noise reduction through a wall; also the sloshing phenomenon can be conveniently studied with the present models;

- to investigate the coupled system behaviour at higher frequency (higher than 300 Hz), combining the FE approach for the structural modeling with other efficient techniques for the acoustic field in order to obtain more accurate solution and reduce the computational cost;

- to extend the study at ultra high frequencies (in the order of thousands Hertz) to completely characterize the problem; although for this frequency range other numerical techniques must be used in order to have reasonable computational cost [42, 43];

- to analyze the effect of lamination for the composite material plate, assuming one flexible wall; this study could be very useful in the aerospace and automotive field where there is a huge use of composite materials.

Data availability

The raw/processed data required to reproduce these findings cannot be shared at this time due to technical limitations.

References

[1] M. Qatu, M. Abdelhamid, J. Pang, and G. Sheng. Overview of automotive noise and vibration. *International Journal of Vehicle Noise and Vibration*, 5, 01 2009.

[2] W. Dobrzynski. Almost 40 years of airframe noise research: What did we achieve? *Journal of Aircraft*, Vol. 47:353 367, 03 2010.

[3] R. Pirk, C. Souto. G. Guimarães, and L. Goes. *Acoustics and Vibro-Acoustics Applied in Space Industry*, page 479 to 512. 08 2013.

[4] N. Atalla, , and R. Bernhard. Review of numerical solutions for low-frequency structural-acoustic problems. *Applied Acoustics*, 43:271–294, 1994.

[5] M. Cinefra. S. Passabì, and E. Carrera. Fem vibroacoustic analysis in the cabin of a regional turboprop aircraft. *Advances in Aircraft and Spacecraft Science*, 5(4):477–498, 2018.

[6] M. Cinefra, A.G. de Miguel, M. Filippi, C. Houriet, A. Pagani, and E. Carrera. Homogenization and free-vibration analysis of elastic metamaterial plates by cuf finite elements. *Mechanics of Advanced Materials and Structures*, 1-10, 2019.

[7] M. Cinefra, G. D'Amico, A. De Miguel Garcia, M. Filippi, A. Pagani, and E. Carrera. Efficient numerical evaluation of transmission loss in homogenized acoustic metamaterials for aeronautical application. *Applied Acoustics*, 164:107253, 2020.

20

[8] S. Danu, N. Saini, Y. Khan, and H. Sharma. Composites for vibro-acoustics-a review. *International Journal of Applied Engineering Research*, 14:6–11, 03 2019.

[9] V. D'Alessandro, G. Petrone, F. Franco, and S. De Rosa. A review of the vibroacoustics of sandwich panels: Models and experiments. *Journal of Sandwich Structures and Materials*, 15:541–582, 09 2013.

[10] D.J. Gorman. Free vibration analysis of the completely free rectangular plate by the method of superposition. *Journal of Sound and Vibration*, 57(3):437 – 447, 1978.

[11] D.J. Gorman and W. Ding. Accurate free vibration analysis of clamped antisymmetric angle-ply laminated rectangular plates by the superposition-galerkin method. *Composite Structures*, 34(4):387 – 395, 1996.

[12] D.J. Gorman and W. Ding. Accurate free vibration analysis of completely free symmetric cross-ply rectangular laminated plates. *Composite Structures*, 60:359–365, 05 2003.

[13] M. Dalaei and A.D. Kerr. Natural vibration analysis of clamped rectangular orthotropic plates. *Journal of Sound and Vibration*, 189(3):399 – 406, 1996.

[14] S.D. Yu and W.L. Cleghorn. Generic free vibration of orthotropic rectangular plates with clamped and simply supported edges. *Journal of Sound and Vibration*, 163(3):439 – 450, 1993.

[15] S. De Rosa, G. Pezzullo, L. Lecce, and F. Marulo. Structural acoustic calculations in the low-frequency range. *Journal of Aircraft*, 31(6):1387–1394, 1994.

[16] S. Dhandole and S. Modak. A comparative study of methodologies for vibro-acoustic fe model updating of cavities using simulated data. *International Journal of Mechanics and Materials in Design*, 6:27–43, 03 2010.

[17] Reza Madjlesi. Application of fem and sea in predicting vibro-acoustic behavior of a flat ribbed panel structure. *Canadian Acoustics*, 35(3):32–33, Sep. 2007.

[18] Jianrun Zhang and Renqiang Jiao. Vibro-acoustic modeling of a rectangular enclosure with a flexible panel in broad range of frequencies and experimental investigations. *Journal of Vibroengineering*, 18(4):2683–2692, jun 2016.

[19] Yunju Yan, Pengbo Li, and Huagang Lin. Analysis and experimental validation of the middle-frequency vibro-acoustic coupling property for aircraft structural model based on the wave coupling hybrid fe-sea method. *Journal of Sound and Vibration*, 371:227 – 236, 2016.

[20] Giuseppe Petrone, Giacomo Melillo, Aurelio Laudiero, and Sergio De Rosa. A statistical energy analysis (sea) model of a fuselage section for the prediction of the internal sound pressure level (spl) at cruise flight conditions. *Aerospace Science and Technology*, 88:340 – 349, 2019.

[21] E. Carrera, M. Cinefra, M. Petrolo, and E. Zappino. *Finite Element Analysis of Structures through Unified Formulation*. John Wiley & Sons, 2014.

[22] G. Li, E. Carrera, M. Cinefra, A.G. de Miguel, A. Pagani, and E. Zappino. An adaptable refinement approach for shell finite element models based on node-dependent kinematics. *Composite Structures*, 210, 11 2018.

[23] D. Chronopoulos, B. Troclet, O. Bareille, and M. Ichchou. Modeling the response of composite panels by a dynamic stiffness approach. *Composite Structures*, 96:111 – 120, 2013.

[24] M. Botshekanan Dehkordi, M. Cinefra, S.M.R. Khalili, and E. Carrera. Mixed lw/esl models for the analysis of sandwich plates with composite faces. *Composite Structures*, 98:330 – 339, 2013.

[25] M.C. Moruzzi, M. Cinefra, and S. Bagassi. Vibroacoustic analysis of an innovative windowless cabin with metamaterial trim panels in regional turboprops. *Mechanics of Advanced Materials and Structures*, 0(0):1–13, 2019.

[26] Z. Liu, M. Fard, and J. Davy. Acoustic properties of the porous material in a car cabin model. 07 2016.

[27] E. Carrera. Multilayered shell theories accounting for layerwise mixed description, part 1: Governing equations. *AIAA Journal*, 37(9):1107–1116, 1999.

[28] E. Carrera and S. Brischetto. Analysis of thickness locking in classical, refined and mixed multi-layered plate theories. *Composite Structures*, 82:549–562, 02 2008.

[29] A.J.M. Ferreira, C.M.C. Roque, E. Carrera, and M. Cinefra. Analysis of thick isotropic and cross-ply laminated plates by radial basis functions and a unified formulation. *Journal of Sound and Vibration*, 330(4):771 – 787, 2011.

[30] E. Carrera, M. Cinefra, G. Li, and G.M. Kulikov. Mitc9 shell finite elements with miscellaneous through-the-thickness functions for the analysis of laminated structures. *Composite Structures*, 154:360 – 373, 2016.

[31] E. Carrera, M. Cinefra, and G. Li. Refined finite element solutions for anisotropic laminated plates. *Composite Structures*, 183:63–76, 2018.

[32] M. Cinefra and E. Carrera. Shell finite elements with different through-the-thickness kinematics for the linear analysis of cylindrical multilayered structures. *International Journal for Numerical Methods in Engineering*, 93:160–182, 2013.

[33] M. Cinefra, E. Zappino, E. Carrera, and S. De Rosa. Fully coupled vibro-acoustic analysis of multi-layered plates by cuf finite elements. Medyna, Italy, 2020. 3rd Euro-Mediterranean Conference on Structural Dynamics and Vibroacoustics.

[34] Q. Zhang and T. Hisada. Studies of the strong coupling and weak coupling methods in fsi analysis. *International Journal for Numerical Methods in Engineering*, 60:2013 – 2029, 07 2004.

[35] M. Cinefra and S. Valvano. A variable kinematic doubly-curved mitc9 shell element for the analysis of laminated composites. *Mechanics of Advanced Materials and Structures*, 23(11):1312–1325, 2016.

[36] R. Srinivasan Puri, D. Morrey, A.J. Bell, J.F. Durodola, E.B. Rudnyi, and J.G. Korvink. Reduced order fully coupled structural acoustic analysis via implicit moment matching. *Applied Mathematical Modelling*, 33(11):4097 – 4119, 2009.

[37] A.W. Leissa. The free vibration of rectangular plates. *Journal of Sound and Vibration*, 31(3):257 – 293, 1973.

[38] P.A.A. Laura, D.V. Bambill, R.E. Rossi, and C.A. Rossit. Vibrations of an orthotropic rectangular plate with a free edge in the case of discontinuously varying thickness. *Journal of Sound and Vibration*, 206(1):109 – 113, 1997.

[39] R.F.S. Hearmon. The frequency of flexural vibration of rectangular orthotropic plates with clamped or supported edges. *Journal of Applied Mechanics*, 26:537–540, 1959.

[40] R.L. Ramkumar, P.C. Chen, and W.J. Sanders. Free vibration solution for clamped orthotropic plates using lagrangian multiplier technique. *AIAA Journal*, 25(1):146–151, 1987.

[41] G. Giunta, F. Biscani, S. Belouettar, and E. Carrera. Hierarchical modelling of doubly curved laminated composite shells under distributed and localised loadings. *Composites Part B: Engineering*, 42(4):682 – 691, 2011.

[42] A. Le Bot. A vibroacoustic model for high frequency analysis. *Journal of Sound and Vibration*, 211(4):537 – 554, 1998.

[43] R.S. Langley and N.S. Bardell. A review of current analysis capabilities applicable to the high frequency vibration prediction of aerospace structures. *The Aeronautical Journal (1968)*, 102(1015):287–297, 1998.

Declaration of interests

☒ The authors declare that they have no known competing financial interests or personal relationships that could have appeared to influence the work reported in this paper.

☐The authors declare the following financial interests/personal relationships which may be considered as potential competing interests:

On behalf of all the authors

Maria Cinefra

Maria Cinefra: Conceptualization, Methodology, Software, Writing - Original Draft, Writing - Review & Editing

Martino Carlo Moruzzi: Software, Validation, Writing - Original Draft

Sara Bagassi: Investigation, Writing - Original Draf

Enrico Zappino: Investigation, Software

Erasmo Carrera: Supervision, Methodology